

Supplementary Information

1 Experimental Section

1.1 Electrode materials preparation

GO was prepared by the method in our previous report.¹ 15 mL GO dispersion liquid (2 mg mL⁻¹), 0.8 mmol Ni(NO₃)₂·6H₂O, 0.8 mmol Co(NO₃)₂·6H₂O (the molar ratio of Ni/Co=1:1) and 3.0 mmol urea were added into 20 mL deionized H₂O. The mixture was kept for stirring for 20 min and then ultrasonicated for 20 min. After that, the mixture was transferred into Teflon-lined stainless-steel autoclave (50 mL) and maintained at 120 °C for 12 h. After cooling to room temperature, the obtained precipitate was collected by centrifugation and rinsed with deionized H₂O five times, and was then dried by freeze drying for 24 h. The obtained sample is named as GO@NiCo-OH. In the subsequent phosphorization, the 100 mg GO@NiCo-OH and 500 mg NaH₂PO₂·H₂O were placed in two separated positions in a flat-bottomed porcelain crucible, where NaH₂PO₂·H₂O was kept at the upstream site of the tube furnace. The tube furnace was heated to 300 °C at a ramping of 5 °C min⁻¹ and maintained for 2 h under the N₂ atmosphere. Before heating process, N₂ is pre-agitated for 20 minutes to remove air from the tube furnace. During heating process, nitrogen is continuously vented into the tube furnace at a rate of 100 ml min⁻¹. After cooling to room temperature, GO@NiCoP and a small quantity of by-product (Na₄P₂O₇ and NaPO₃) were obtained. To obtain pure GO@NiCoP, the sample obtained by the above procedure was added into 200 mL deionized H₂O and stirred at room temperature for 24 h. After that, the sample was collected by suction filtration and washed with deionized H₂O, and was then dried by freeze drying for 24 h. The sample is named as GO@NiCoP. The Ni/Co molar ratios were altered by adjusting the molar ratio of Ni²⁺/Co²⁺ of 4:0, 3:1, 1:3 and 0:4 in the starting materials. The obtained

hydroxides are named as GO@Ni-OH, GO@Ni₃Co₁-OH, GO@Ni₁Co₃-OH and GO@Co-OH. The obtained phosphides are named as GO@NiP, GO@Ni₃Co₁P, GO@Ni₁Co₃P and GO@CoP.

1.2 Materials characterization

The microstructure and lattice information were obtained by Auriga FIB/SEM (Zeiss, Germany) with an acceleration voltage of 5 kV and Libra 200 HRTEM (Zeiss, Germany) with an acceleration voltage of 200 kV. Phase composition was recorded by D/max-2500 X-ray diffraction (Rigaku Cooperation, Japan) from 5 to 80° at a scan rate of 4° min⁻¹. Elements and valence states were determined by ESCALAB 250Xi (Thermo Fisher, USA) X-ray photoelectron spectrometer (Al K α , 1486.6 eV) from 0 to 1350 eV. Functional groups were recorded by Nicolet iS5 Fourier transfer infrared spectrophotometer (Thermo Fisher, USA) and a LabRAM HR Evolution spectrophotometer (HORIBA Scientific, France) with an operating wavelength of 632.8 nm. Specific surface area and porosity were recorded by Gemini VII 2390 (Micromeritics Instrument, USA).

1.3 Density functional theory computation

The CASTE package of Materials Studio were performed to present the DFT-based first-principles calculations.² In the DFT calculations, the generalized gradient approximation (GGA) in the form of PW91^{3, 4} was adopted, and the final set of energies for all calculations was computed with an energy cut off of 750 eV. With the crystal cell parameter from the experimental XRD results, a 2×2×1 supercell single layer with 200 Å vacuum space is constructed, then the geometry optimization is performed. All atoms were fully relaxed until the residual forces on each atom are smaller than 0.03 meV Å⁻¹,¹⁵ and the convergence criteria for energy is set to be 10⁻⁵ eV. The Brillouin zone integration was performed with 3×3×1 Γ-centered Monkhorst-Pack k-point meshes in geometry optimization⁶. The adsorption energy was defined as: $E_{\text{adsorption}} = E_{\text{adsorbate/substrate}} - E_{\text{adsorbate}} - E_{\text{substrate}}$ and the deprotonation energy was

defined as: $E_{\text{deprotonation}} = E_{\text{defect}} - E_{\text{perfect}} + 0.5E_{\text{H}_2}$.

1.4 Electrochemical measurements

The electrochemical performance of these samples was tested by CHI760E electrochemical workstation (Chenhua, China). The freshly prepared 3 M KOH, saturated calomel electrode and platinum electrode ($1.5 \times 1.5 \text{ cm}^2$) were used for the electrolyte, reference electrode and counter electrode, respectively. The work electrode ($1 \times 1 \text{ cm}^2$) with $1.5 \sim 2.0 \text{ mg}$ active materials was prepared by the method in our previous report.⁷ Cyclic voltammetry (CV) measurements were tested at the potential window from $-0.1 \sim 0.5 \text{ V}$ with different scan rate and the galvanostatic charge-discharge (CC) measurements were tested at the potential window from $-0.1 \sim 0.4 \text{ V}$ with different current density. The electrochemical impedance spectroscopy (EIS) was conducted at the frequency range of $0.01 \sim 100 \text{ kHz}$ at steady-state open circuit potential with a perturbation of 5 mV . The specific capacitance ($C_m, \text{ F g}^{-1}$) and specific capacity ($Q, \text{ mAh g}^{-1}$) of the electrodes were obtained from the CC curves by the equations respectively:

$$C_m = \frac{I \times \Delta t}{m \times \Delta V} \quad (1)$$

$$Q = \frac{I \times \Delta t}{3.6 \times m} \quad (2)$$

wherein I (A), Δt (s), m (g) and ΔV (V) represent the discharge current, discharge time, mass of active materials and potential window (Deducting the IR drop), respectively.

To fabricate the asymmetric supercapacitor (ASC) device, the active material was used as the positive electrode and the active graphene (AG) was used as the negative electrode. The specific capacitance ($C, \text{ F g}^{-1}$), the energy density ($E, \text{ Wh kg}^{-1}$) and power density ($P, \text{ W kg}^{-1}$) were determined by the following equations:

$$C = \frac{I \times \Delta t}{m \times \Delta V} \quad (3)$$

$$E = \frac{C \Delta V^2}{7.2} \quad (4)$$

$$P = \frac{3600E}{\Delta t} \quad (5)$$

wherein I (A), Δt (s), m (g) and ΔV (V, deducting the IR drop) represent the discharge current, discharge time, total mass of positive and negative materials and potential window. The mass ratio of positive and negative materials was determined by the following equation:

$$\frac{m^+}{m^-} = \frac{C^- \times \Delta V^-}{C^+ \times \Delta V^+} \quad (6)$$

wherein m^+ (g), C^+ (F g⁻¹), ΔV^+ (V, deducting the IR drop) is the mass, specific capacitance, potential window of the positive materials; m^- (g), C^- (F g⁻¹), ΔV^- (V, deducting the IR drop) is the mass, specific capacitance, potential window of the negative materials.

Fig. S1. The SEM image of (a) GO@Ni-OH, (b) GO@Ni₃Co₁-OH, (c) GO@NiCo-OH, (d) GO@Ni₁Co₃-OH, (e) GO@Co-OH, (f) NiCoP.

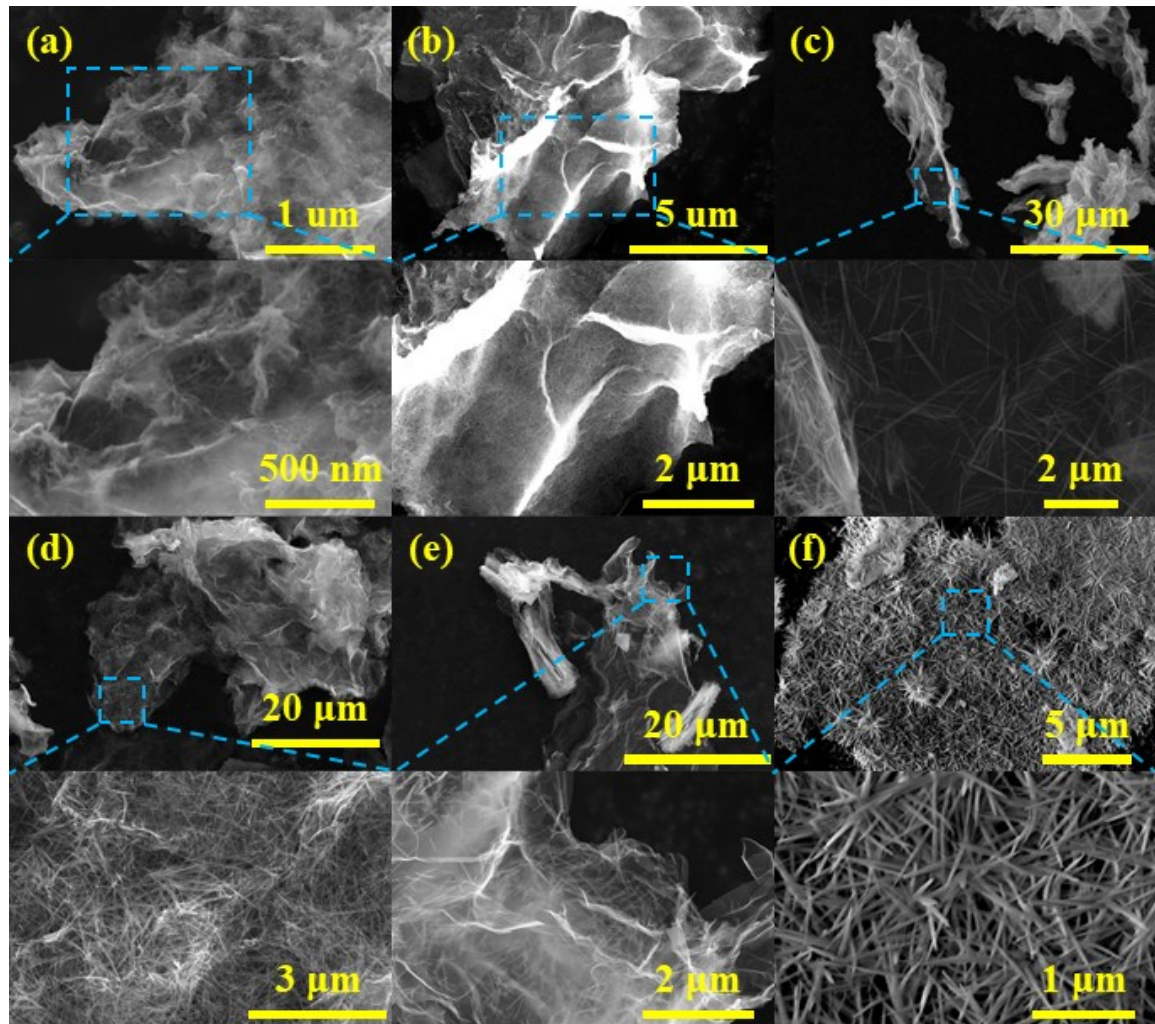


Fig. S2. The XRD pattern of NiCoP.

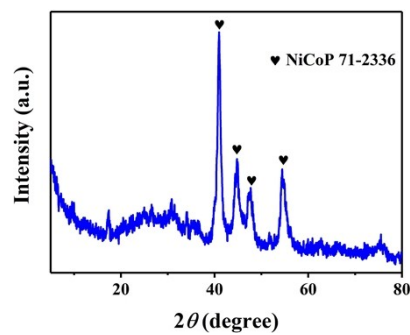


Fig. S3. (a) The CC curves of GO@NiP at the different current densities of 2-20 A g⁻¹, (b) the CC

curves of GO@NiCoP at the different current densities of 2-60 A g⁻¹, (c) the rate capability of GO@NiCoP.

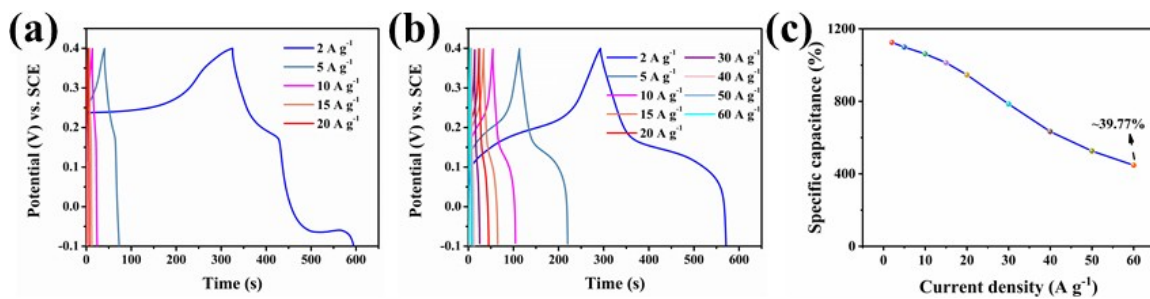
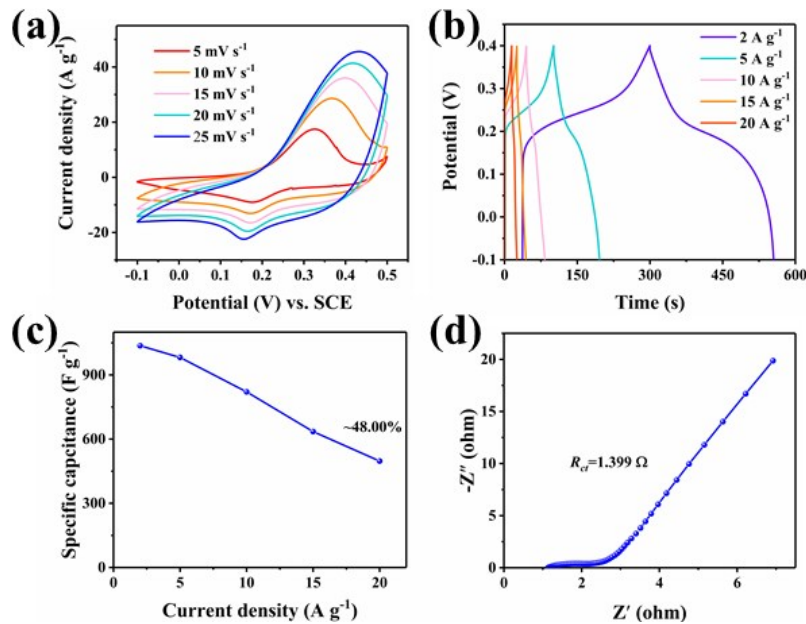


Fig. S4. (a) The CV curves, (b) CC curves, (c) rate capability, (d) Nyquist plot of NiCoP.



References

- 1 C. Jing, Y. Huang, L. Xia, Y. Chen, X. Wang, X. Liu, B. Dong, F. Dong, S. Li and Y. Zhang, *Appl. Surf. Sci.*, 2019, 143700.
- 2 A. Inc., *Journal*, 2001.
- 3 B. Delley, *J. Chem. Phys.*, 1990, **92**, 508-517.
- 4 A. Bhattacharya, S. Bhattacharya, C. Majumder and G. Das, *Phys. Rev. B*, 2011, **83**, 033404.
- 5 H. Lv, H. Gao, Y. Yang and L. Liu, *Appl. Catal. A-Gen*, 2011, **404**, 54-58.
- 6 J. Li, Z. Liu, Q. Zhang, Y. Cheng, B. Zhao, S. Dai, H.-H. Wu, K. Zhang, D. Ding and Y. Wu, *Nano Energy*, 2019, **57**, 22-33.
- 7 C. Jing, X. Guo, L. Xia, Y. Chen, X. Wang, X. Liu, B. Dong, F. Dong, S. Li and Y. Zhang, *Chem. Eng. J.*, 2020, **379**, 122305.

